tvst

https://doi.org/10.1167/tvst.8.3.28

Article

Automated Measurement of the Foveal Avascular Zone in Swept-Source Optical Coherence Tomography Angiography Images

Hirokazu Ishii[1], Takuhei Shoji[1], Yuji Yoshikawa[1], Junji Kanno[1], Hisashi Ibuki[1], and Kei Shinoda[1]

[1] Department of Ophthalmology, Saitama Medical University, Saitama, Japan

Correspondence: Takuhei Shoji, Department of Ophthalmology, Saitama Medical University, 38 Morohongo Moroyama-machi, Iruma, Saitama 350-0495, Japan. e-mail: shoojii@gmail.com

Received: 11 December 2018
Accepted: 14 March 2019
Published: 30 May 2019

Keywords: automated measurement; foveal avascular zone; swept-source optical coherence tomography; optical coherence tomography angiography images

Citation: Ishii H, Shoji T, Yoshikawa Y, Kanno J, Ibuki H, Shinoda K. Automated measurement of the foveal avascular zone in swept-source optical coherence tomography angiography images. Trans Vis Sci Tech. 2019;8(3):28, https://doi.org/10.1167/tvst.8.3.28

Purpose: The purpose of this study was to evaluate automated measurement of the foveal avascular zone (FAZ) area using the Kanno-Saitama macro (KSM) software in Image J with swept-source optical coherence tomography angiography (SS-OCTA) images.

Methods: In this cross-sectional study, one photographer scanned the macular area (3 $\times$ 3 mm) of healthy volunteers twice on the same day, at the same time. The FAZ area was measured from the en face image of the superficial retinal layer by two masked examiners, using the KSM and the Advanced Retina Imaging (ARI)-network method in Carl Zeiss online analysis. Intra- and interscan reproducibility and FAZ area were compared among the methods.

Results: Forty eyes of 22 healthy volunteers were included in the analysis. The mean $\pm$ SD age of the subjects was 34.6 $\pm$ 12.4 years. Intra- and interscan intraclass coefficients ranged from 0.997 to 1.000 and 0.989 to 0.995, respectively. The mean FAZ area was 0.264 $\pm$ 0.08 mm^2 by the KSM, 0.245 $\pm$ 0.08 mm^2 by the ARI, and 0.281 $\pm$ 0.09 mm^2 by the manual method. The mean difference between the KSM and manual methods was 0.015 mm^2, which was significantly smaller than the mean difference between the ARI and manual methods (0.034 mm^2; $P < 0.001$).

Conclusions: Automated determination of the FAZ area is feasible and yields results comparable to those obtained by manual measurement. The FAZ area measured with the KSM program is less user dependent and could potentially contribute to our understanding of the pathophysiology of various retinal diseases, particularly underlying vascular diseases.

Translational Relevance: This study demonstrates a novel automated determination of the FAZ area using the Image J macro program in SS-OCTA images. This program was feasible and yields results comparable to those obtained by manual measurement.

Introduction

The foveal avascular zone (FAZ) is the avascular area of the central macula; it demonstrates large individual variations in size and shape.[1] The FAZ area is highly sensitive to ischemic events and can be an indicator of several pathologic processes. FAZ has long been studied as an indicator of vasculature change in the retina. Bresnick et al.[2] reported in 1984 that FAZ dimensions are strongly positively correlated with the severity of capillary nonperfusion in the posterior retina in eyes with proliferative diabetic retinopathy.

Previous studies have reported enlarged FAZ areas in retinal ischemic diseases, such as diabetic retinopathy (DR)[3] and retinal vascular obstruction (RVO)[4]; a decreased FAZ area in retinopathy of prematurity[5]; decreased vessel density in DR and glaucoma[6]; lower fractal dimensions in RVO,[4] DR,[3] and uveitis eyes[7]; increased vessel diameter index in RVO[4] and DR[3];

and decreased FAZ circularity in glaucoma[8] and DR.[3] These studies have demonstrated that quantitative optical coherence tomography angiography (OCTA) metrics may provide useful information for the diagnosis of ocular diseases. In addition, structural changes occur in the FAZ due to DR, branch retinal vein occlusion, and talc retinopathy.[9–11]

Previous studies used fluorescein angiography, but a number of reports using OCTA have been published. OCTA has allowed noninvasive evaluation of the retinal and choroidal vascular circulation without the need for dye injection.[12,13] OCTA has increasingly gained popularity and has been applied to a broad spectrum of disease.[14–21] In addition, an association between glaucoma and FAZ structure has been reported,[8,22] and the importance of evaluating FAZ structure by OCTA is increasingly recognized.

The FAZ area, however, has typically been manually measured and only some OCTA machines are equipped with automated measurement software. Although the FAZ area value is clinically useful, most reports have defined a boundary manually or semiautomatically, in which the examiner has to plot all endpoints of vascular signals in the macular area.[23] While previous reports showed no statistically difference in the FAZ area value between manual and automated measurements when using the AngioVue OCTA instrument software of the RTVue XR Avanti (Optovue, Inc., Fremont, CA),[24] the manual measurement method is limited in that it is subjective in determining how many end points should be plotted or which points should be selected as end points. Moreover, when using the FAZ area in a clinical study, a single examiner should measure and plot the FAZ area, which is difficult in large study cohorts. An automated program may thus offer a better approach for analyzing FAZ area in a large number of subjects.

We therefore investigated whether it would be feasible to quantify the FAZ area by using an automated image analysis technique that would be reproducible, less sensitive to user interaction, and could reduce the time required for analysis. Thus, we evaluated application of a new macro-based automated method for analysis of the FAZ area using ImageJ software (developed by Wayne Rasband; http://rsb.info .nih.gov/ij/index.html, provided in the public domain by the National Institutes of Health, Bethesda, MD) with swept-source OCTA (SS-OCTA) and compared the FAZ areas obtained by automated measurements and manual measurements.

Materials and Methods

Study Population

This cross-sectional study of healthy subjects was approved by the Ethics Committee of Saitama Medical University and was conducted in accordance with the tenets of the Declaration of Helsinki. Healthy subjects were included if they were 20 years of age or older, fulfilled the eligibility requirements detailed below, and signed an informed consent form between October 2017 and November 2017.

Healthy subjects were recruited from the ophthalmology outpatient clinic of Saitama Medical University Hospital (Saitama, Japan). All participants underwent a comprehensive ophthalmic examination, including slit-lamp biomicroscopy, measurement of intraocular pressure (IOP) by noncontact tonometry (Tonoref II; Nidek Co., Ltd., Aichi, Japan), fundus photography (CX-1; Canon, Inc., Tokyo, Japan). Axial length and central corneal thickness were measured (Optical Biometer OA-2000; Tomey Corp., Nagoya, Japan). Automated visual field (VF) assessment was performed using an algorithm (24-2 Swedish Interactive Thresholding Algorithm; Carl Zeiss Meditec, Jena, Germany). Retinal nerve fiber layer measurements were made using spectral-domain OCT (SD-OCT) (Spectralis OCT; Heidelberg Engineering, Heidelberg, Germany), and SS-OCTA (Plex Elite 9000; Carl Zeiss Meditec, Jena, Germany).

The exclusion criteria included the following: (1) participants aged under 20 years, (2) reflective error more than +3.0 diopters or less than −6.0 diopters, (3) axial length exceeding 26 mm, (4) nerve fiber layer thinning outside of the normal limit, (5) evidence of other ocular diseases, DR, retinal vein/artery occlusion, age-related macular degeneration, retinal detachment, tilted disc, exfoliation syndrome, high myopia and ocular neuropathy without mild ametropia, and (6) poor image quality (signal strength <8 due to signal noise; 1 = minimum, 10 = maximum).

OCT Angiography

A 3 × 3-mm (1024 × 1024 pixels) OCTA image centered on the fovea was scanned using SS-OCTA (Plex Elite 9000, Version 1.6.0.21130; Carl Zeiss Meditec Dublin, CA); SS-OCTA featured a central wavelength of 1060 nm, an A-scan rate of 100,000 scans per second, and an axial and transverse tissue resolution of 6 and 20 μm, respectively. The angiography image was processed by using both

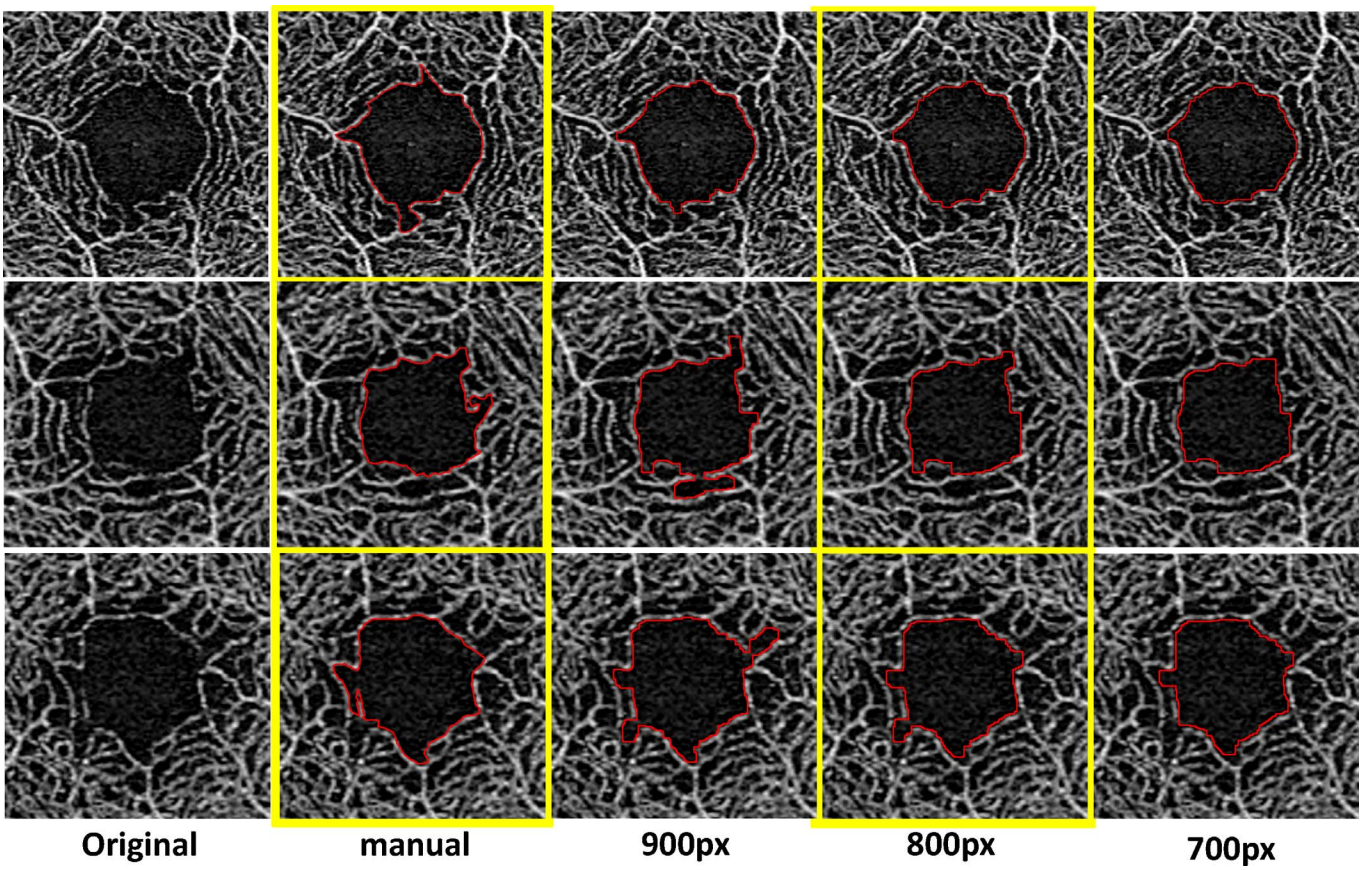

Figure 1. Effect of downsizing on the final FAZ area boundary using macro program. First column (*left*), original images; second column, drew the FAZ area manually; third to fifth column, after downsize to 900. With 800 or 700 pixels, the FAZ area was drawn automatically.

phase/Doppler shift and amplitude variation (Optical Micro-Angiography).[25] All OCTA scans were performed with enhanced depth imaging (EDI) methods for all patients, twice a day.

The built-in software in SS-OCTA generates en face images from slabs at different layers by automated segmentation. The superficial retinal layer was defined as follows: the inner boundary is the internal limiting membrane layer and the outer boundary is an approximation of the inner plexiform layer.

OCTA Image Processing

To determine the edge points and border of the FAZ area, we used three different methods, described below, and compared the FAZ area and circularity determined with each of these methods.

The Kanno-Saitama Macro (KSM) Program

The KSM program is an automated analysis program using the ImageJ macro that we devised, which can extract the FAZ area automatically. This requires correct determination of the FAZ area by making up for capillary ring disruptions constituting the FAZ. First, we downsized the images to delineate the boundary line smoothly. Figure 1 shows the representative results. The KSM macro reduced the obtained en face image from 1024 × 1024 to 800 × 800 pixels. Second, we performed image processing by binarization and skeletonization. More than 20 binarization methods are available in the ImageJ macro. Figure 2 shows the representative binarization methods such as those by Li,[26] Otsu,[27] and Phansalkar.[28] Among them, we used the Li[26] method for binarization. Subsequently, we made up for capillary ring disruption by repeating *dilate* for the purpose of enlarging the region and *erode* for narrowing it. The number of erode and dilation repetitions was determined after several trials (Fig. 2). Finally, we returned image size to the original, extracted the region showing FAZ disruption, and enlarged the region for 2 pixels. The detailed code is shown below. All images were analyzed using the

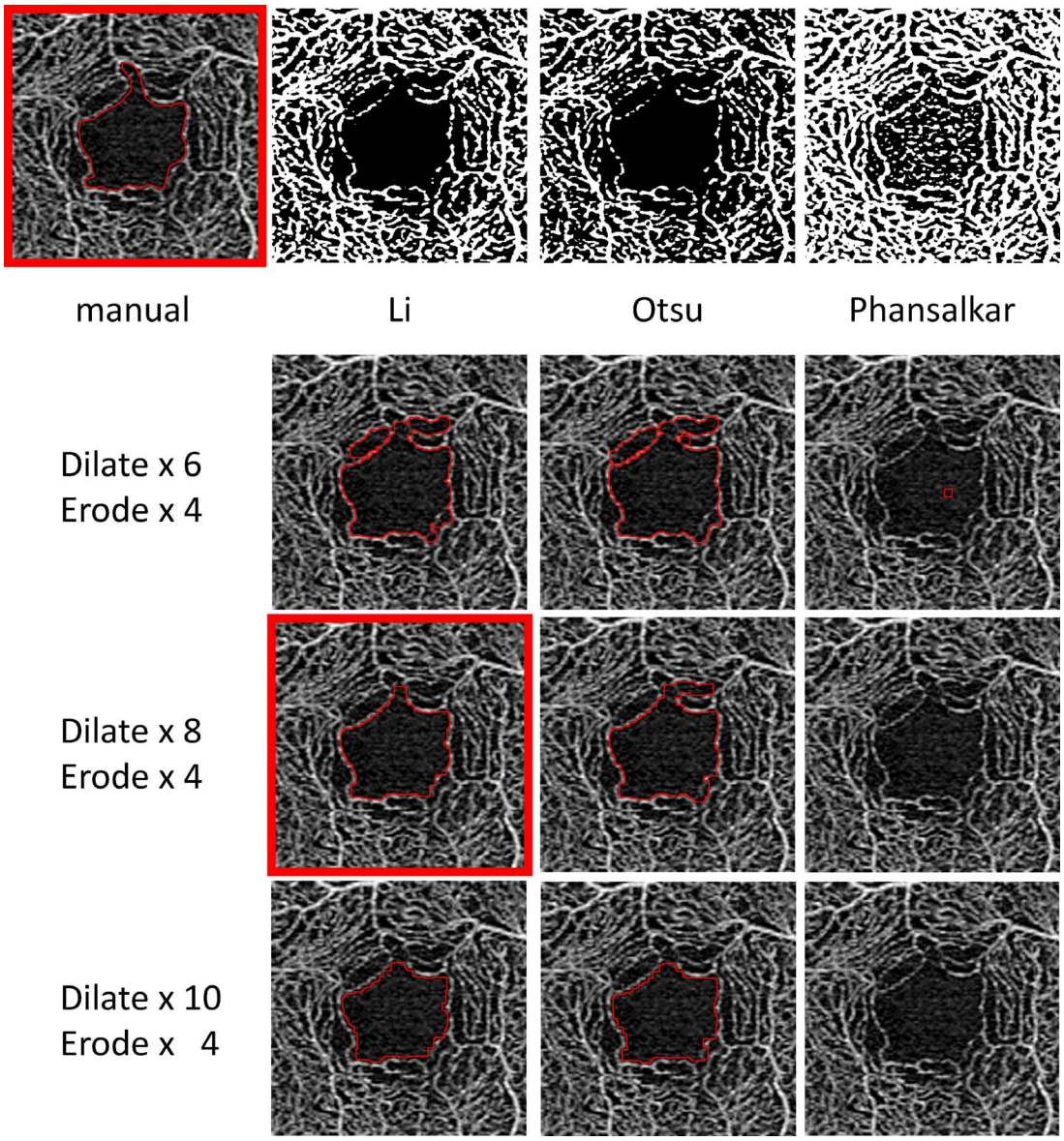

Figure 2. Manually and automatically drawn FAZ boundary after using several representative binarization methods. Li[26] seems to be the most reliable among binarization methods.

same ImageJ macro.

```
run("Size...", "width=800 height=800 constrain average interpolation=Bilinear");
run("Auto Threshold...", "method=Li white");
setOption("BlackBackground", true);
run("Skeletonize");
run("Dilate"); *8 times repeat
run("Erode"); *4 times repeat
run(''Size...'', ''width=1024 height=1024 constrain average interpolation=Bilinear");
doWand(512, 512);
run("Enlarge...", "enlarge=2 pixels");
roiManager("Add");
```

The image-processing algorithm is illustrated in Figure 3.

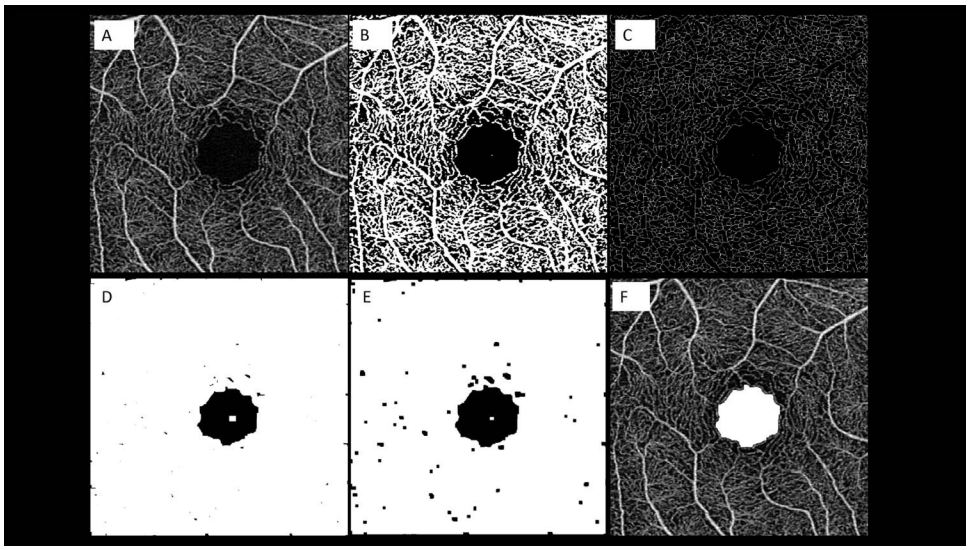

Figure 3. Representation of the algorithm used to process the images. The images of the superficial capillary plexus (SCP) were first imported in ImageJ software. After running the *erode* command on the en face image, which we acquired in 800 × 800 pixels (A), we performed binarization (B) and skeletonization (C). Subsequently, we repeated the *dilate* command for connecting capillary ring disruption (D) and repeated the *erode* command for narrowing vessels (E). Finally, we returned the image size to normal and extracted the FAZ line (F).

Advanced Retina Imaging (ARI) Zeiss Macular Algorithm v 0.6.1

The ARI network is a prototype, proprietary algorithm available in Carl Zeiss online analysis that extracts the FAZ boundary and allows quantification of FAZ area at the superficial capillary plexus (SCP) in the macular area. Anonymized raw files were downloaded from the Zeiss PLEX Elite 9000 instruments and uploaded in the ARI network portal. En face angiograms were then exported in Portable Network Graphics format.

Manual Measurements

In the manual method, two masked examiners (H. Ishii and H. Ibuki) independently drew the FAZ area contour point by point on all en face images. The examiners used the scale parameter of the software, which was set to define a 1024-pixel width in the images as 3 mm.

Measurement of FAZ Area With OCTA

The FAZ area was defined as the area denoted by the connected points along the borderline of the identifiable capillary network in the parafoveal area. The FAZ area (in square millimeters) was calculated using ImageJ software.

Testing Protocol

Each participant was scanned twice. In the first scans, we repeated measurements twice using the three methods to calculate intrascan reproducibility (repeatability). In the second scans, we also performed measurements using the three methods. Interscan reproducibility was calculated using the first measurements obtained in the first and second scans for each method. To compare the FAZ area across the different methods, the average value of the first and second scans was determined. In the manual measurements, the mean value of the first measurements of first scan and second scan was used. The final manual value was the average of the mean value of each examiner.

Statistical Analysis

The data for continuous variables are expressed as the mean value and standard deviation (mean ± SD). We evaluated intra- and interscan reproducibility of the FAZ area for the three methods. Intra- and interscan reproducibilities were summarized as the intraclass correlation coefficient (ICC) and coefficient of variation (CV) between measurements, respectively. We used the paired *t*-test and Bland-Altman plots to compare the FAZ area among the three methods.

Table 1. Ocular and Systemic Characteristic of This Study

No. of Patients (*n*)	22
Age (years)	34.6 ± 12.4
Sex (male / female)	18 / 22
No. of eyes (*n*)	40
BCVA (Log MAR)	−0.08 ± 0.00
CCT (μm)	525.6 ± 31.1
IOP (mmHg)	14.1 ± 3.02
Spherical equivalent (diopters)	−1.84 ± 1.90
Axial length (mm)	24.2 ± 0.81
Mean deviation (dB)	−0.29 ± 1.53
Pattern standard deviation (dB)	1.67 ± 0.81
Systolic blood pressure (mmHg)	118.6 ± 10.2
Diastolic blood pressure (mmHg)	75.9 ± 10.8
Heart rate (beat/mean)	72.7 ± 9.7
Self-reported history of hypertension, *n* (%)	1, (4.6)
Self-reported history of dyslipidemia, *n* (%)	1, (4.6)
Self-reported history of diabetes, *n* (%)	0, (0)
Self-reported history of cardiovascular disorders, *n* (%)	0, (0)
Antihypertensive medication, *n* (%)	0, (0)
Diabetes medication, *n* (%)	0, (0)
Smoking history, *n* (%)	4, (18.2)
Drinking history, *n* (%)	6, (27.3)

Values are expressed as mean ± standard deviation. BCVA, best corrected visual acuity; CCT, central corneal thickness; IOP, intra-ocular pressure.

The differences between manual measurements and KSM and ARI were also compared.

A P value <0.05 was considered to indicate a statistically significant difference. All statistical analyses were performed using software (JMP version 10.1; SAS Institute Inc., Cary, NC).

Results

Forty-four eyes of 22 healthy participants were enrolled; four eyes were excluded from analysis, as one eye showed an retinal nerve fiber layer thickness outside the normal limit and three eyes had poor image quality. Thus, 40 eyes from 22 participants were eligible for analysis. The subjects' ocular and systemic characteristics are described in Table 1. The mean age of the patients was 34.6 ± 12.4 years (mean ± SD), best corrected visual acuity was −0.08 ± 0.00, axial length was 24.2 ± 0.81 mm, spherical equivalent was −1.84 ± 1.90 diopter, IOP was 14.1 ± 3.0 mm Hg, central corneal thickness was 525.6 ± 31.1 μm, and mean deviation was −0.29 ± 1.53 dB. Four subjects (18.2%) had a history of smoking, six subjects (27.3%) had a history of drinking, and one subject (4.6%) had a history of hypertension. There was no history of hypertension, diabetes, or cardiovascular disease.

Intra- and Interscan Reproducibility of the FAZ Area

Figure 4 shows a representative case of this study. In this case, the FAZ areas calculated by examiners 1 and 2, using the KSM and ARI methods, were 0.329 mm^2, 0.320 mm^2, 0.310 mm^2, and 0.291 mm^2, respectively. It took about 1 minute per scan to extract the FAZ area manually because it required more than 40 edge points. In contrast, it took less than 1 second per scan to extract the FAZ area by running the KSM program. Table 2 shows the intra- and interscan reproducibility. For the intrascan reproducibility of the FAZ area, the manual methods had excellent and comparable ICC values, and both the ARI and KSM program had perfect reproducibility. For the interscan reproducibility, all the methods showed excellent ICC values of more than 0.989, and the CV value ranged from 2.1% to 2.9%. These values were comparable among methods.

Difference Between the Automated and Manual Measurements

Figure 5 shows the scatterplots comparing the manual measurements and those obtained by ARI and KSM, respectively. Measurements of the FAZ area with both the ARI and KSM methods were smaller than those obtained by manual measurements. Figure 6 shows the Bland-Altman plots between the manual, ARI, and KSM measurements. The FAZ area obtained with manual measurements were larger than those obtained using the ARI and KSM methods. Additionally, the FAZ area obtained using the KSM method was larger than that obtained with the ARI method. Table 3 compares the differences between the areas obtained by ARI and manual methods and between those obtained with the KSM and manual methods. The FAZ area obtained with the KSM method was more similar to that

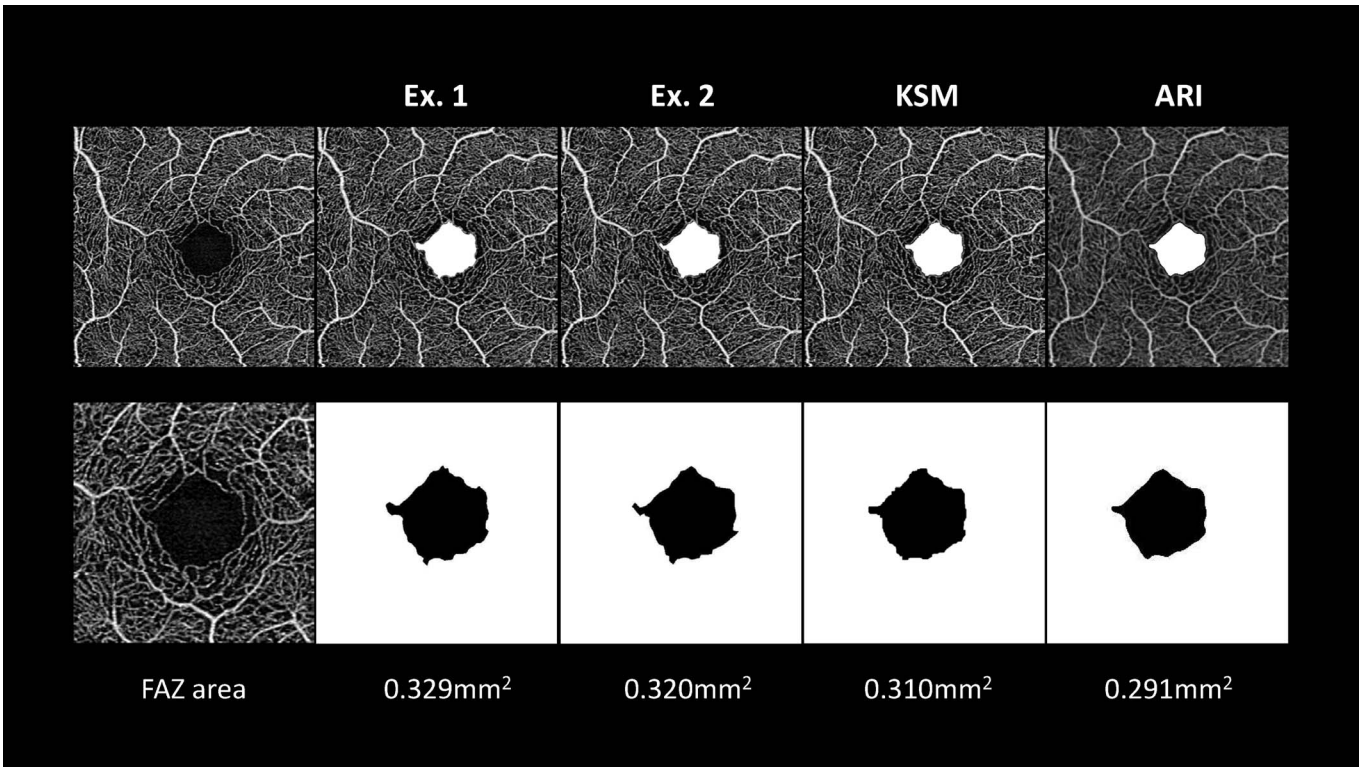

Figure 4. A representative participant was a 24-year-old healthy female. Examiners 1 and 2 extracted the boundary manually. The FAZ area of examiners 1 and 2 were 0.329 and 0.320 mm^2, respectively. Both the KSM and ARI methods determined the boundary automatically. The FAZ area determined by the KSM and ARI methods was 0.310 mm^2 and 0.291 mm^2, respectively.

Table 2. Intra- and Inter-Scan Reproducibility of Foveal Avascular Zone Area

	Intra-Scan			Inter-Scan		
Method	FAZ Area (mm^2)	ICC (95% CI)	CV (%) (95% CI)	FAZ Area (mm^2)	ICC (95% CI)	CV (%) (95% CI)
Manual (Examiner 1)	Examination 1: 0.280 ± 0.087 Examination 2: 0.281 ± 0.087	0.999 (0.998 to 1.00)	0.5 (0.3 to 0.7)	Scan 1: 0.280 ± 0.087 Scan 2: 0.283 ± 0.088	0.994 (0.989 to 0.997)	2.1 (1.5 to 2.7)
Manual (Examiner 2)	Examination 1: 0.274 ± 0.087 Examination 2: 0.276 ± 0.086	0.997 (0.995 to 0.998)	1.5 (1.2 to 1.9)	Scan 1: 0.274 ± 0.087 Scan 2: 0.277 ± 0.088	0.989 (0.980 to 0.994)	2.9 (2.3 to 3.6)
ARI	Examination 1: 0.244 ± 0.081 Examination 2: 0.244 ± 0.081	1 (1.00 to 1.00)	0	Scan 1: 0.244 ± 0.081 Scan 2: 0.245 ± 0.082	0.995 (0.990 to 0.997)	2.2 (1.7 to 2.8)
KSM	Examination 1: 0.264 ± 0.084 Examination 2: 0.264 ± 0.084	1 (1.00 to 1.00)	0	Scan 1: 0.264 ± 0.084 Scan 2: 0.263 ± 0.085	0.993 (0.987 to 0.996)	2.4 (1.8 to 3.0)

Values of the foveal avascular zone (FAZ) area are expressed as mean ± standard deviation. ICC, intra-class correlation; CV, coefficient of variation.

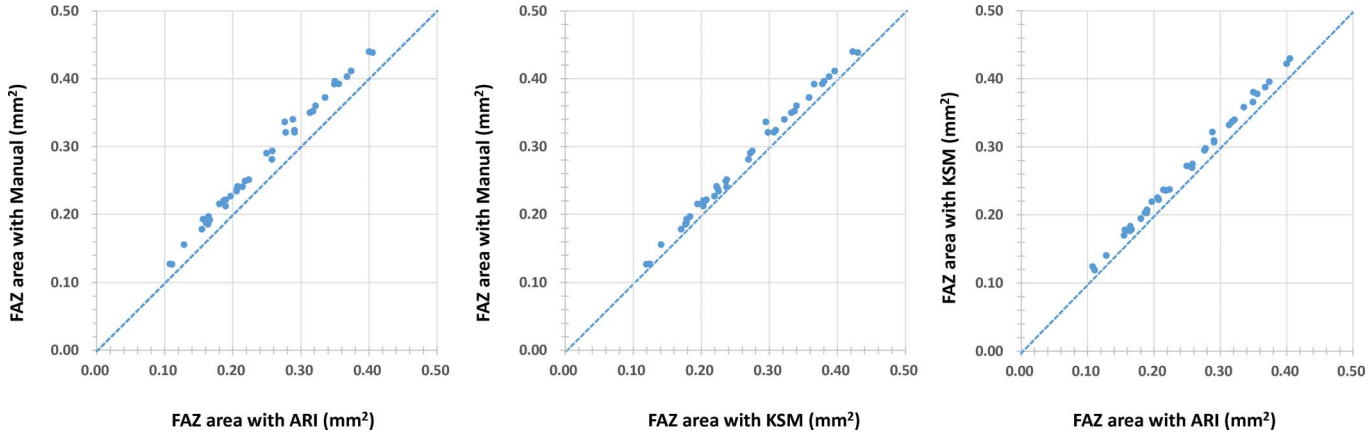

Figure 5. Scatterplots showing the relationship of each measurement such as manual, ARI, and KSM methods.

obtained by manual methods than were those obtained with ARI ($P = 0.001$, paired t-test).

Discussion

We here evaluated the performance of a novel automated lateral-segmentation technique, called the KSM method, that we specifically designed for quantification of the FAZ. The program showed high reproducibility, implying that this automated technique may be useful for characterizing the size and contour of the FAZ area. Moreover, the difference in the FAZ area obtained with the KSM program and manually was significantly smaller than that between the area obtained with the ARI and manual methods. These results suggested that the KSM program yielded results closer to manual measurements than did the ARI.

To our knowledge, the FAZ area has not been

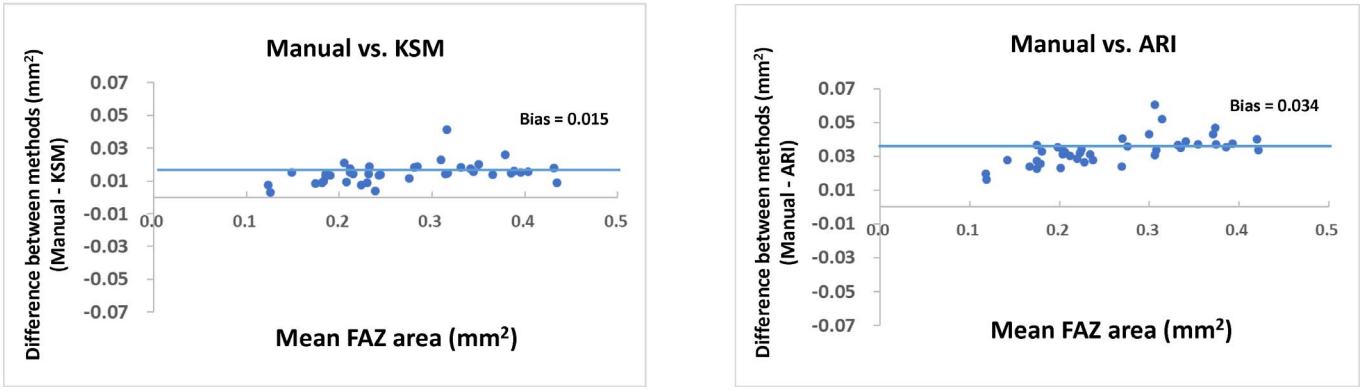

Figure 6. Bland-Altman plots showing the relationship between the measurements obtained using manual, ARI, and KSM methods.

Table 3. Comparison Between Differences Between the ARI and Manual Methods and Those Between the KSM and Manual Methods

Methods	Difference of Average FAZ Area (mm^2)	*P* Value[a]
Manual - KSM	0.015 ± 0.006	<0.001
Manual - ARI	0.034 ± 0.008	

KSM, Kanno-Saitama macro; ARI, advanced retina imaging; FAZ, foveal avascular area.

[a] Paired *t*-test.

compared among manual methods and an automated program provided by the manufacturer (ARI) or the ImageJ macro program (KSM) using the PLEX Elite, a new SS-OCTA device. The KSM program is custom-written in ImageJ macro script language and has the advantages of being low cost and time-saving and has easy availability, accessibility, and utility. The FAZ is surrounded by interconnected capillary beds.[29] The KSM program involves dilating the vessel to connect the central capillary after skeletonizing. These processes seem reasonable for defining the FAZ area and results in a shape similar to that obtained manually (Fig. 2).

The mean FAZ area in our cohort was generally comparable to previous reports. Table 4 shows the range of FAZ areas measured in various studies with different OCTA instruments. The mean FAZ area (3 × 3 mm) in our cohort ranged from 0.244 to 0.288 mm^2, which is greater than the 0.17 mm^2 reported by Hwang et al.,[30] the 0.23 mm^2 reported by Linderman et al.,[31] the 0.233 mm^2 reported by Chen et al,[32] and the 0.22 to 0.27 mm^2 reported by La Spina et al.[33] It is lower than the 0.29 mm^2 reported by Iafe et al.[23] and is comparable to the 0.25 mm^2 reported by Carpineto et al,[34] the 0.25 to 0.28 mm^2 reported by Shahlaee et al.,[35] the 0.27 to 0.29 mm^2 reported by Magrath et al.,[24] and the 0.28 mm^2 reported by Coscas et al.[36] In general, the FAZ area varies significantly among individuals,[37] and these differences could be due to differences in sex, age, axial length, and/or racial distribution. Linderman et al.[31] indicated that the FAZ area was increased in females and that there was a negative correlation between axial length and FAZ area, which is likely due to the differences in ocular magnification across eyes. Moreover, Shiihara et al. reported that, although the interinstrument correlation coefficients were also high for the superficial FAZ, the absolute value of the FAZ area differed significantly among instruments with a significant fixed bias. Thus, these differences among studies might be due to participant and instrument factors.

Another strength of the current study was that we automatically measured FAZ area using commercially available SS-OCTA. Table 4 also shows that most of previous studies used the RTVue XR Avanti, one of the first commercially available OCTA devices, which used a split-spectrum amplitude-decorrelation angiography reconstruction algorithm. La Spina et al.[33] reported that automated software in the RTVue XR Avanti provided significantly larger areas than manual analysis, and consequently, the interclass automated/manual correlation coefficient was rather weak (0.689).[33] In contrast, Linderman et al.[31] reported that FAZ area for manual segmentation was greater than automatic segmentation. Regarding the comparison between instruments, Corvi et al. reported that the mean superficial FAZ area obtained with the RTVue XR Avanti (0.221 mm^2) and with Plex Elite (0.225 mm^2) was similar for manual measurements. In this study, automated software provided by the manufacturer (ARI) yielded significantly smaller areas than did those obtained by manual analysis. Although the reason for this difference remains unknown, it may be related to the different lateral segmentation boundaries of algorithms employed in OCTA devices. Whereas mean difference of 0.015 mm^2 between manual and KSM program might be minim in clinical practice, studies comparing measurements from different methods (i.e., manual versus auto) should be evaluated carefully.

FAZ area measurements using OCTA has also gained increased popularity and has been applied to a broad spectrum of diseases. Previous reports have shown that the larger FAZ area in the superficial plexus were positively correlated with lower visual acuity in eyes after diabetic macular edema was resolved[39] and improved visual acuity after macular edema resolution with intravitreal aflibercept for eyes with central RVO, which is associated with a smaller FAZ area in both the superficial and deep plexi.[40] These findings suggested that microvascular ischemic changes in the macular area lead to FAZ enlargement, which might reflect the severity of photoreceptor damage. Kitagawa et al.[41] reported that the FAZ area expanded after epiretinal membrane surgery, and Kita et al.[42] reported that macular hole closure after vitrectomy leads to a significant decrease in the size of the FAZ area. Thus, the FAZ area was affected not only by microvascular ischemic changes, but also

Table 4. Past Publications of Foveal Avascular Zone (FAZ) Area Measurements Using Optical Coherence Tomography Angiography (OCTA)

First Author (Reference)	Number	Mean Age (Years)	Device	Measurements Method	Mean FAZ Area ± SD (mm^2)
Corvi[38]	Healthy 18 subjects 36 eyes	28.1 ± 3.8	[1] RTVue XR Avanti [2] Spectralis [3] AngioPlex [4] Prototype PlexElite [5] RS-3000 [6] OCT-HS100 [7] Redo NX	Superficial Manual	[1] 0.2211 ± 0.1002 [2] 0.2408 ± 0.1141 [3] 0.2319 ± 0.1097 [4] 0.2250 ± 0.1004 [5] 0.2372 ± 0.1082 [6] 0.2394 ± 0.1137 [7] 0.2575 ± 0.1263
La Spina[33]	Healthy 24 subjects 24 eyes	27.0 ± 9.0	RTVue XR Avanti	Superficial Manual Auto (built-in software)	Manual: 0.215 ± 0.06 Auto: 0.268 ± 0.05
Shahlaee[37]	Healthy 17 subjects 34 eyes	38.0	RTVue XR Avanti	Superficial Manual	Examiner 1: 0.25 ± 0.096 Examiner2: 0.28 ± 0.106
Carpineto[34]	Healthy 60 subjects 60 eyes	28.9 ± 7.6	RTVue XR Avanti	Superficial Auto	Examiner1: 0.251 ± 0.097 Examiner2: 0.252 ± 0.097
Iafe[23]	Healthy 70 subjects 113 eyes	48 ± 20	RTVue XR Avanti	Superficial Manual	0.289 ± 0.108
Garrity[45]	Healthy 95 subjects 152 eyes	42 ± 25	RTVue XR Avanti	Superficial Auto	0.270 ± 0.101
Falavarjani[46]	Healthy 70 subjects 70 eyes	42.8 ± 17.2	RTVue XR Avanti	Superficial Manual	0.32 ± 0.11
Liu[47]	Healthy 87 subjects 174 eyes	38.7 ± 15.9	RTVue XR Avanti	Superficial Auto	Right eye: 0.33 ± 0.11 Left eye: 0.33 ± 0.12
Samara[48]	Healthy 67 subjects 70 eyes	42	RTVue XR Avanti	Superficial Manual	0.266 ± 0.097
Linderman[31]	Healthy 116 subjects 116 eyes	30.5 ± 14.5	RTVue XR Avanti	Manual Semi-auto Auto (full retina)	Manual: 0.257 ± 0.104 Semi-auto: 0.231 ± 0.0939 Auto: 0.234 ± 0.0933
Mihailovic[49]	Healthy 24 subjects 24 eyes	30.6 ± 12.1	[1] RTVue XR Avanti [2] OCT-HS100 [3] Spectralis	Superficial Manual	[1] 0.312 ± 0.090 [2] 0.298 ± 0.090 [3] 0.329 ± 0.095
Linderman[50]	Healthy 175 subjects 350 eyes	27.9 ± 11.9	Cirrus HD-OCT	Superficial Manual	0.278 ± 0.101
Shiihara[51]	Healthy 27 subjects 27 eyes	36.8 ± 10.2	[1] DRI Triton [2] RS 3000 advance [3],[4] Cirrus HD-OCT 5000	Superficial Manual [[1]–[3]] Auto [[4]]	[1] 0.264 ± 0.071 [2] 0.278 ± 0.072 [3] 0.257 ± 0.066 [4] 0.253 ± 0.068

Table 4. Continued

First Author (Reference)	Number	Mean Age (Years)	Device	Measurements Method	Mean FAZ Area ± SD (mm^2)
Magrath[24]	Healthy 25 subjects 50 eyes	33	[1],[2] RTVue XR Avanti [3] Cirrus HD-OCT 5000	Superficial Auto [[1]) Manual [[2],[3])	[1] 0.2855 [2] 0.2739 [3] 0.26572
Kulikov[52]	Healthy 36 subjects 36 eyes	51.2 ± 11.5	REVO	Full retina Manual	0.33 ± 0.1

Semi-auto, semi-automated; auto, automated.

macular structural changes, with horizontal or vertical traction. Additionally, Choi et al.[22] reported that the size of the FAZ area was increased in glaucoma patients, while Kwon et al.[8] reported that glaucoma eyes with a central VF defect had particularly larger FAZ areas. Thus, evaluation of the FAZ area both in a cross-sectional and longitudinal study is relevant to understanding the pathogenesis and severity of various retinal diseases.

There are several limitations to this study. First, this is a preliminary study, in which we evaluated only relatively young, healthy, Asian subjects. Wagner-Schuman et al.[43] reported that African Americans have significantly larger foveal pits than do Caucasian individuals. In addition, although Manalastas et al.[44] reported that reproducibility of OCTA was comparable between healthy and glaucoma patients, all subjects in our study had normal vision, resulting in subjectively good image quality and minimal motion artifacts, which might cause overestimation of the results. Thus, further studies with a larger sample size and larger age range may be needed.

In conclusion, our automated ImageJ-based method for determining the FAZ area was comparable to manual methods and showed values that were more similar to those obtained by manual measurement than were the currently available ARI automated measurements. This study showed that automated determination of the FAZ area is feasible and yielded results comparable to manual measurement. The FAZ area measured with the KSM program may save time, prove to be less user dependent, and could potentially contribute to our understanding of the pathophysiology of various retinal diseases, particularly those with underlying vascular involvement.

Acknowledgments

Supported by the Daiwa Securities Health Foundation (Tokyo, Japan), Takeda Science Foundation (Tokyo, Japan), Grant-in-Aid for Young Researchers in Saitama Medical University Hospital (Saitama, Japan), and a Japan Society for the Promotion of Science grant (KAKENHI Grants 15K21335 and 16KK0208).

Disclosure: **H. Ishii**, None; **T. Shoji**, Alcon (F); **Y. Yoshikawa**, None; **J. Kanno**, None; **H. Ibuki**, None; **K. Shinoda**, None

References

1. Chui TY, VanNasdale DA, Elsner AE, Burns SA. The association between the foveal avascular zone and retinal thickness. *Invest Ophthalmol Vis Sci*. 2014;55:6870–6877.
2. Bresnick GH, Condit R, Syrjala S, Palta M, Groo A, Korth K. Abnormalities of the foveal avascular zone in diabetic retinopathy. *Arch Ophthalmol*. 1984;102:1286–1293.
3. Tang FY, Ng DS, Lam A, et al. Determinants of quantitative optical coherence tomography angiography metrics in patients with diabetes. *Sci Rep*. 2017;7:2575.
4. Koulisis N, Kim AY, Chu Z, et al. Quantitative microvascular analysis of retinal venous occlusions by spectral domain optical coherence tomography angiography. *PLoS One*. 2017;12:e0176404.

5. Mintz-Hittner HA, Knight-Nanan DM, Satriano DR, Kretzer FL. A small foveal avascular zone may be an historic mark of prematurity. *Ophthalmology*. 1999;106:1409–1413.
6. Rao HL, Pradhan ZS, Weinreb RN, et al. Regional comparisons of optical coherence tomography angiography vessel density in primary open-angle glaucoma. *Am J Ophthalmol*. 2016;171:75–83.
7. Kim AY, Rodger DC, Shahidzadeh A, et al. Quantifying retinal microvascular changes in uveitis using spectral-domain optical coherence tomography angiography. *Am J Ophthalmol*. 2016;171:101–112.
8. Kwon J, Choi J, Shin JW, Lee J, Kook MS. Glaucoma diagnostic capabilities of foveal avascular zone parameters using optical coherence tomography angiography according to visual field defect location. *J Glaucoma*. 2017; 26:1120–1129.
9. Wang Q, Chan S, Yang JY, et al. Vascular density in retina and choriocapillaris as measured by optical coherence tomography angiography. *Am J Ophthalmol*. 2016;168:95–109.
10. Conrath J, Giorgi R, Raccah D, Ridings B. Foveal avascular zone in diabetic retinopathy: quantitative vs qualitative assessment. *Eye (Lond)*. 2005;19:322–326.
11. Friberg TR, Gragoudas ES, Regan CD. Talc emboli and macular ischemia in intravenous drug abuse. *Arch Ophthalmol*. 1979;97:1089–1091.
12. Jia Y, Tan O, Tokayer J, et al. Split-spectrum amplitude-decorrelation angiography with optical coherence tomography. *Opt Express*. 2012; 20:4710–4725.
13. Spaide RF, Klancnik JM Jr., Cooney MJ. Retinal vascular layers imaged by fluorescein angiography and optical coherence tomography angiography. *JAMA Ophthalmol*. 2015;133:45–50.
14. Freiberg FJ, Pfau M, Wons J, Wirth MA, Becker MD, Michels S. Optical coherence tomography angiography of the foveal avascular zone in diabetic retinopathy. *Graefes Arch Clin Exp Ophthalmol*. 2016;254:1051–1058.
15. de Carlo TE, Chin AT, Bonini Filho MA, et al. Detection of microvascular changes in eyes of patients with diabetes but not clinical diabetic retinopathy using optical coherence tomography angiography. *Retina*. 2015;35:2364–2370.
16. Al-Sheikh M, Akil H, Pfau M, Sadda SR. Swept-source OCT angiography imaging of the foveal avascular zone and macular capillary network density in diabetic retinopathy. *Invest Ophthalmol Vis Sci*. 2016;57:3907–3913.
17. Takase N, Nozaki M, Kato A, Ozeki H, Yoshida M, Ogura Y. Enlargement of foveal avascular zone in diabetic eyes evaluated by en face optical coherence tomography angiography. *Retina* 2015;35:2377–2383.
18. Adhi M, Filho MA, Louzada RN, et al. Retinal capillary network and foveal avascular zone in eyes with vein occlusion and fellow eyes analyzed with optical coherence tomography angiography. *Invest Ophthalmol Vis Sci*. 2016;57: OCT486–494.
19. Balaratnasingam C, Inoue M, Ahn S, et al. Visual acuity is correlated with the area of the foveal avascular zone in diabetic retinopathy and retinal vein occlusion. *Ophthalmology*. 2016; 123:2352–2367.
20. Di G, Weihong Y, Xiao Z, et al. A morphological study of the foveal avascular zone in patients with diabetes mellitus using optical coherence tomography angiography. *Graefes Arch Clin Exp Ophthalmol* 2016;254:873–879.
21. Kashani AH, Lee SY, Moshfeghi A, Durbin MK, Puliafito CA. Optical coherence tomography angiography of retinal venous occlusion. *Retina*. 2015;35:2323–2331.
22. Choi J, Kwon J, Shin JW, Lee J, Lee S, Kook MS. Quantitative optical coherence tomography angiography of macular vascular structure and foveal avascular zone in glaucoma. *PLoS One*. 2017;12:e0184948.
23. Iafe NA, Phasukkijwatana N, Chen X, Sarraf D. Retinal capillary density and foveal avascular zone area are age-dependent: quantitative analysis using optical coherence tomography angiography. *Invest Ophthalmol Vis Sci*. 2016;57: 5780–5787.
24. Magrath GN, Say EAT, Sioufi K, Ferenczy S, Samara WA, Shields CL. Variability in foveal avascular zone and capillary density using optical coherence tomography angiography machines in healthy eyes. *Retina* 2017;37:2102–2111.
25. Bojikian KD, Chen CL, Wen JC, et al. Optic disc perfusion in primary open angle and normal tension glaucoma eyes using optical coherence tomography-based microangiography. *PLoS One*. 2016;11:e0154691.
26. Li CH, Tam PKS. An iterative algorithm for minimum cross entropy thresholding. *Pattern Recognit Lett*. 1998;19:771–776.

27. Otsu N. A threshold selection method from gray-level histograms. *IEEE transactions on systems, man, and cybernetics*. 1979;9:62–66.
28. Phansalkar N, More S, Sabale A, Joshi M. Adaptive local thresholding for detection of nuclei in diversity stained cytology images. *Communications and Signal Processing (ICCSP), 2011 International Conference on: IEEE*; 2011:218–220.
29. Tick S, Rossant F, Ghorbel I, et al. Foveal shape and structure in a normal population. *Invest Ophthalmol Vis Sci*. 2011;52:5105–5110.
30. Hwang TS, Zhang M, Bhavsar K, et al. Visualization of 3 distinct retinal plexuses by projection-resolved optical coherence tomography angiography in diabetic retinopathy. *JAMA Ophthalmol*. 2016;134:1411–1419.
31. Linderman R, Salmon AE, Strampe M, Russillo M, Khan J, Carroll J. Assessing the Accuracy of foveal avascular zone measurements using optical coherence tomography angiography: segmentation and scaling. *Trans Vis Sci Tech*. 2017;6:16.
32. Chen FK, Menghini M, Hansen A, Mackey DA, Constable IJ, Sampson DM. Intrasession repeatability and interocular symmetry of foveal avascular zone and retinal vessel density in OCT angiography. *Trans Vis Sci Tech*. 2018;7:6.
33. La Spina C, Carnevali A, Marchese A, Querques G, Bandello F. Reproducibility and reliability of optical coherence tomography angiography for foveal avascular zone evaluation and measurement in different settings. *Retina*. 2017;37:1636–1641.
34. Carpineto P, Mastropasqua R, Marchini G, Toto L, Di Nicola M, Di Antonio L. Reproducibility and repeatability of foveal avascular zone measurements in healthy subjects by optical coherence tomography angiography. *Br J Ophthalmol* 2016;100:671–676.
35. Shahlaee A, Samara WA, Hsu J, et al. In vivo assessment of macular vascular density in healthy human eyes using optical coherence tomography angiography. *Am J Ophthalmol*. 2016;165:39–46.
36. Coscas F, Sellam A, Glacet-Bernard A, et al. Normative data for vascular density in superficial and deep capillary plexuses of healthy adults assessed by optical coherence tomography angiography. *Invest Ophthalmol Vis Sci*. 2016;57:OCT211–223.
37. Shahlaee A, Pefkianaki M, Hsu J, Ho AC. Measurement of foveal avascular zone dimensions and its reliability in healthy eyes using optical coherence tomography angiography. *Am J Ophthalmol*. 2016;161:50–55 e51.
38. Corvi F, Pellegrini M, Erba S, Cozzi M, Staurenghi G, Giani A. Reproducibility of vessel density, fractal dimension, and foveal avascular zone using 7 different optical coherence tomography angiography devices. *Am J Ophthalmol*. 2018;186:25–31.
39. Moein HR, Novais EA, Rebhun CB, et al. Optical coherence tomography angiography to detect macular capillary ischemia in patients with inner retinal changes after resolved diabetic macular edema. *Retina;* 2018;38:2277–2284.
40. Winegarner A, Wakabayashi T, Hara-Ueno C, et al. Retinal microvasculature and visual acuity after intravitreal aflibercept in eyes with central retinal vein occlusion: an optical coherence tomography angiography study. *Retina*. 2018;38:2067–2072.
41. Kitagawa Y, Shimada H, Shinojima A, Nakashizuka H. Foveal avascular zone area analysis using optical coherence tomography angiography before and after idiopathic epiretinal membrane surgery. *Retina*. 2019;39:339–346.
42. Kita Y, Inoue M, Kita R, et al. Changes in the size of the foveal avascular zone after vitrectomy with internal limiting membrane peeling for a macular hole. *Jpn J Ophthalmol*. 2017;61:465–471.
43. Wagner-Schuman M, Dubis AM, Nordgren RN, et al. Race- and sex-related differences in retinal thickness and foveal pit morphology. *Invest Ophthalmol Vis Sci*. 2011;52:625–634.
44. Manalastas PIC, Zangwill LM, Saunders LJ, et al. Reproducibility of optical coherence tomography angiography macular and optic nerve head vascular density in glaucoma and healthy eyes. *J Glaucoma* 2017;26:851–859.
45. Garrity ST, Iafe NA, Phasukkijwatana N, Chen X, Sarraf D. Quantitative analysis of three distinct retinal capillary plexuses in healthy eyes using optical coherence tomography angiography. *Invest Ophthalmol Vis Sci*. 2017;58:5548–5555.
46. Falavarjani KG, Shenazandi H, Naseri D, et al. Foveal avascular zone and vessel density in healthy subjects: an optical coherence tomography angiography study. *J Ophthalmic Vis Res*. 2018;13:260–265.
47. Liu G, Keyal K, Wang F. Interocular symmetry of vascular density and association with central macular thickness of healthy adults by optical

coherence tomography angiography. *Sci Rep*. 2017;7:16297.
48. Samara WA, Say EA, Khoo CT, et al. Correlation of foveal avascular zone size with foveal morphology in normal eyes using optical coherence tomography angiography. *Retina*. 2015;35:2188–2195.
49. Mihailovic N, Brand C, Lahme L, et al. Repeatability, reproducibility and agreement of foveal avascular zone measurements using three different optical coherence tomography angiography devices. *PLoS One*. 2018;13:e0206045.
50. Linderman RE, Muthiah MN, Omoba SB, et al. Variability of foveal avascular zone metrics derived from optical coherence tomography angiography images. *Trans Vis Sci Tech*. 2018;7:20.
51. Shiihara H, Sakamoto T, Yamashita T, et al. Reproducibility and differences in area of foveal avascular zone measured by three different optical coherence tomographic angiography instruments. *Sci Rep*. 2017;7:9853.
52. Kulikov AN, Maltsev DS, Burnasheva MA. Improved analysis of foveal avascular zone area with optical coherence tomography angiography. *Graefes Arch Clin Exp Ophthalmol*. 2018;256:2293–2299.